

Electronic Supplementary Information (SI) for

Integration of ultrathin and modified NiCoAl-layered double hydroxide nanosheets with N-doped reduced graphene oxide for high-performance all-solid-state supercapacitors

Fei Liu,^a Yuyun Chen,^b Ying Liu,^a Jianchun Bao,^a Min Han,^{*a} and Zhihui Dai^{*a}

^a Jiangsu Key Laboratory of Biofunctional Materials, School of Chemistry and Materials Science, Nanjing Normal University, Nanjing 210023, P. R. China

^b School of Chemistry and Chemical Engineering, Guangxi University for Nationalities, Nanning 530008, P. R. China

*To whom correspondence should be addressed.

Email: 07203@njnu.edu.cn (Prof. M. Han);

daizhihui@njnu.edu.cn (Prof. Z. Dai)

Tel/Fax: +86-25-85891051

This information contains:

- (1) Digital photographs for m-LDH/NRG NHs, pure m-LDH and NRG dispersions (Figure S1)
- (2) The HAADF-STEM images for pure NiCoAl-LDH and m-LDH nanosheets as well as m-LDH/NRG NHs (**Figure S2**)
- (3) The mapping analysis for N element in the m-LDH/NRG (**Figure S3**)
- (4) Raman for NiCoAL-LDH, m-LDH and m-LDH/NRG at 200 to 1000 cm⁻¹ (**Figure S4**)
- (5) Raman for NRG and m-LDH/NRG at 1100 to 1900 cm⁻¹ (**Figure S5**)
- (6) The survey XPS spectrum for m-LDH/NRG NHs (**Figure S6**)
- (7) Fine core-level XPS spectra of NiCoAl-LDH (**Figure S7**)
- (8) Fine core-level XPS spectra of m-LDH (**Figure S8**)
- (9) N₂ sorption isothermal plots for m-LDH/NRG NHs and NiCoAl-LDH nanosheets (**Figure S9**)

(10) CV plots for m-LDH/NRG NHs, NRG and pure Ni foam at a constant potential scan rate, and CV plots for m-LDH/NRG NHs, NiCoAl-LDH and m-LDH and at different potential scan rates (**Figure S10**)

(11) The detailed data for XPS spectra of m-LDH/NRG NHs, pure m-LDH and unmodified NiCoAl-LDH nanosheets (**Table S1**)

(12) ICP data for pure NiCoAl-LDH and m-LDH nanosheets (**Table S2**)

(13) The detailed integral areas of O1s peaks for NiCoAl-LDH and m-LDH nanosheets (**Table S3**)

(14) Comparing the electrochemical performance of m-LDH/NRG NHs with other reported electrode materials (**Table S4**)

(15) References

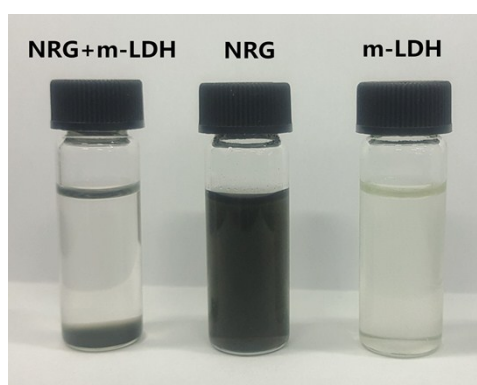


Fig. S1 Digital photographs for the dispersions of m-LDH/NRG NHs as well as pure m-LDH and NRG dispersions.

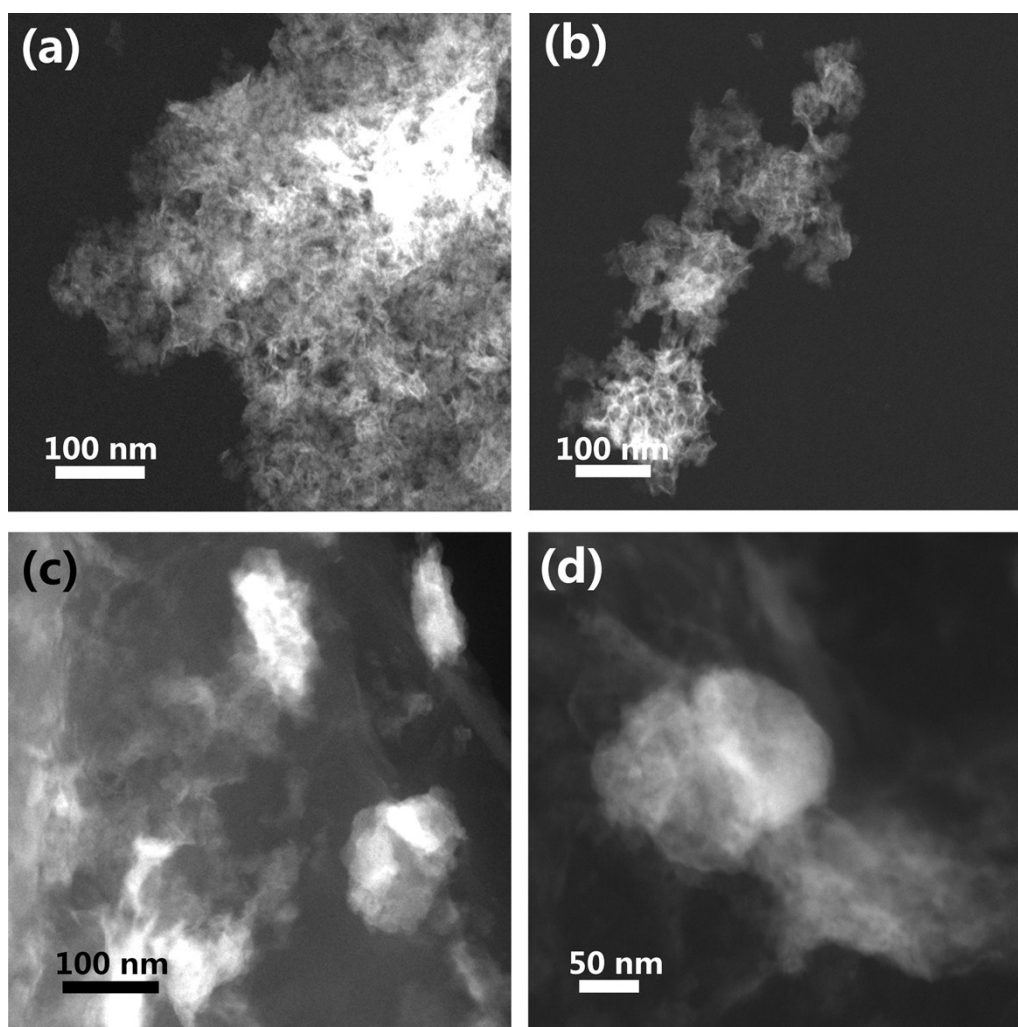


Fig. S2 (a-b) Low-magnification HAADF-STEM images of NiCoAl-LDH (a) and m-LDH (b) nanosheets. (c-d) Low and high-magnification HAADF-STEM images for m-LDH/NRG NHs.

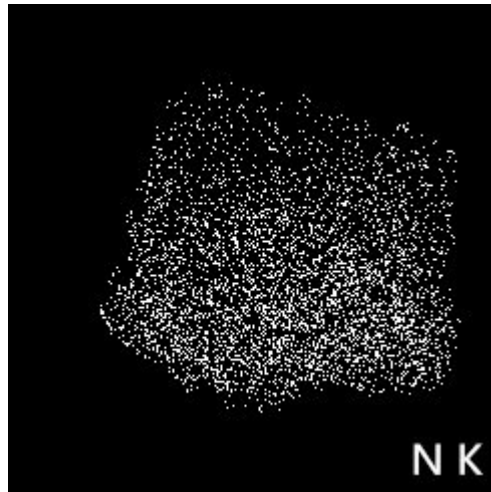


Fig. S3 The mapping analysis for N element in the m-LDH/NRG NHs.

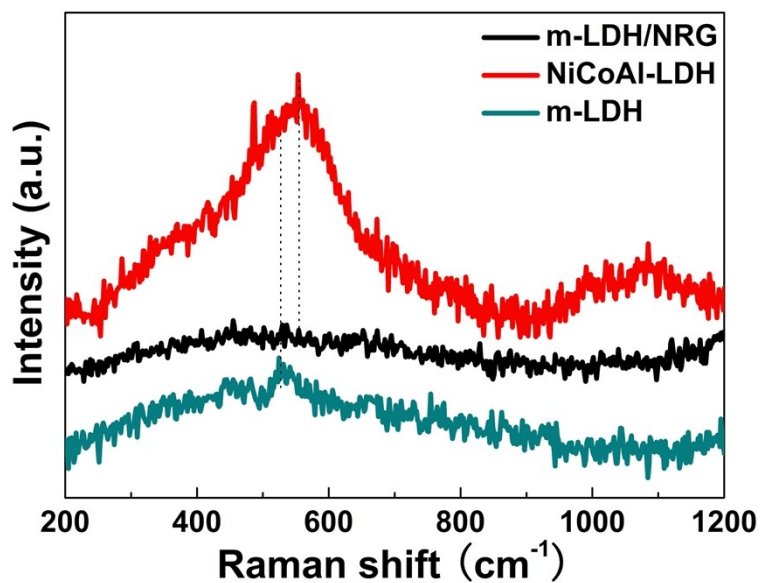


Fig. S4 Comparing the Raman spectra of m-LDH/NRG NHs, NiCoAl-LDH and m-LDH nanosheets at the low wavenumber region (ranging from 200 to 1100 cm⁻¹).

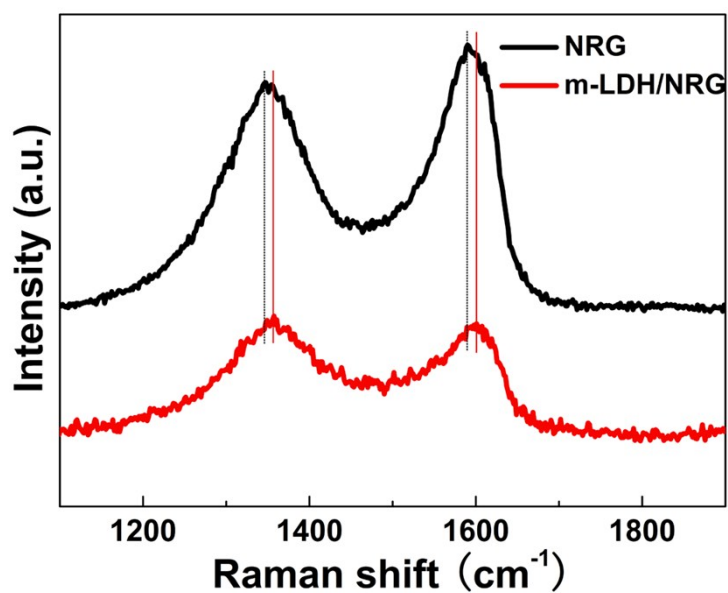


Fig. S5 Comparing the Raman spectra of m-LDH/RGN NHs and pure m-LDH nanosheets at the high wavenumber region (ranging from 1100 to 1900 cm⁻¹).

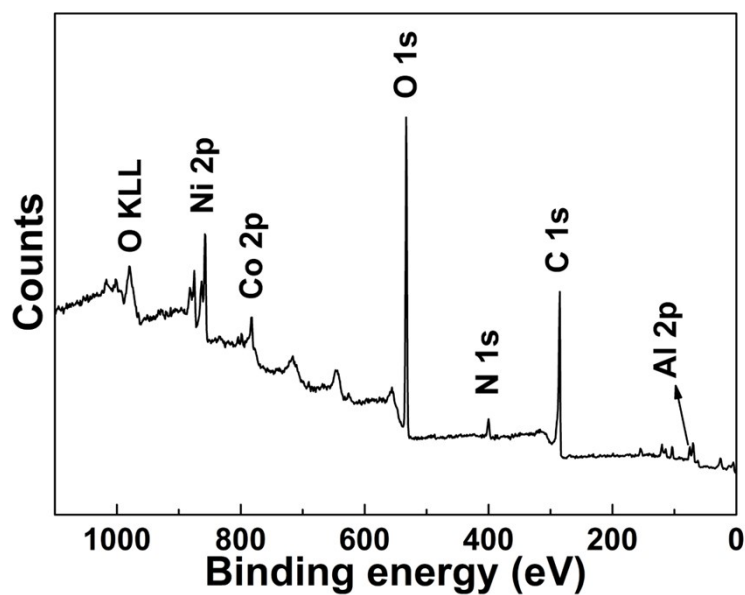


Fig. S6 The survey XPS spectrum for m-LDH/NRG NHs.

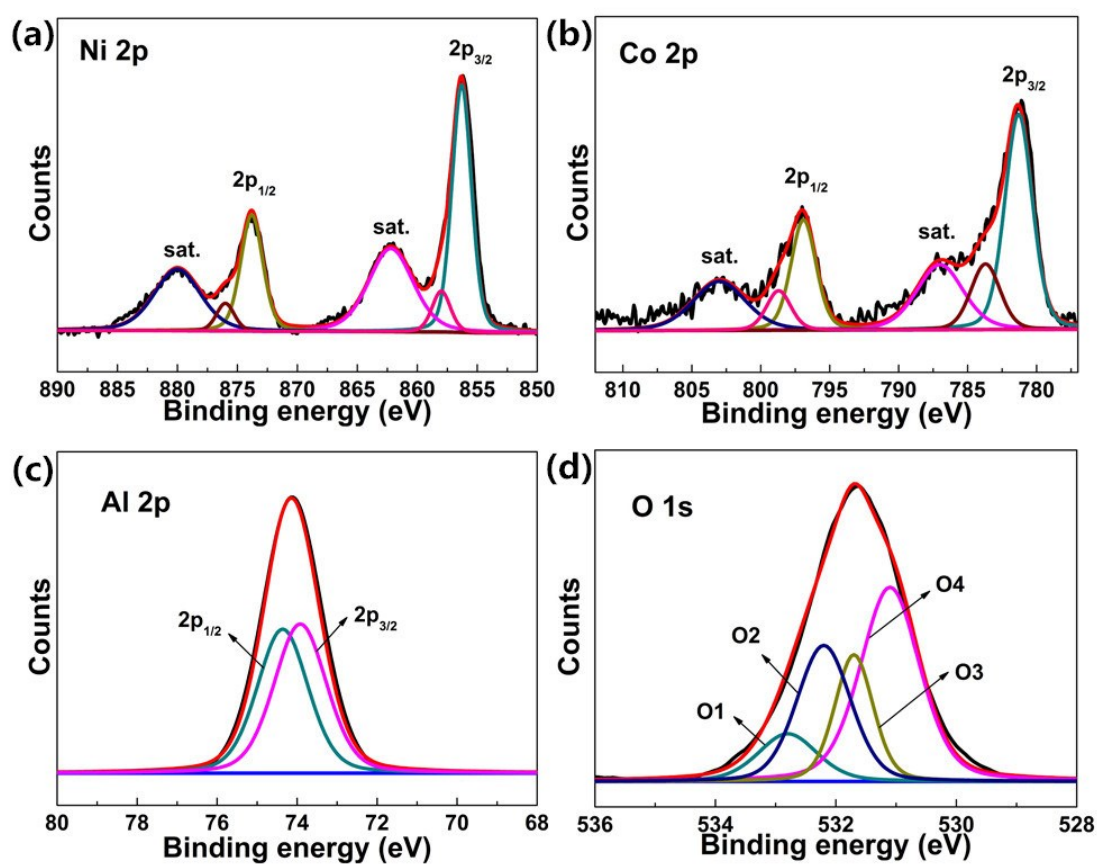


Fig. S7 Fine core-level XPS spectra for Ni 2p (a), Co 2p (b), Al 2p (c) and O 1s(d) peaks of the unmodified NiCoAl-LDH nanosheets.

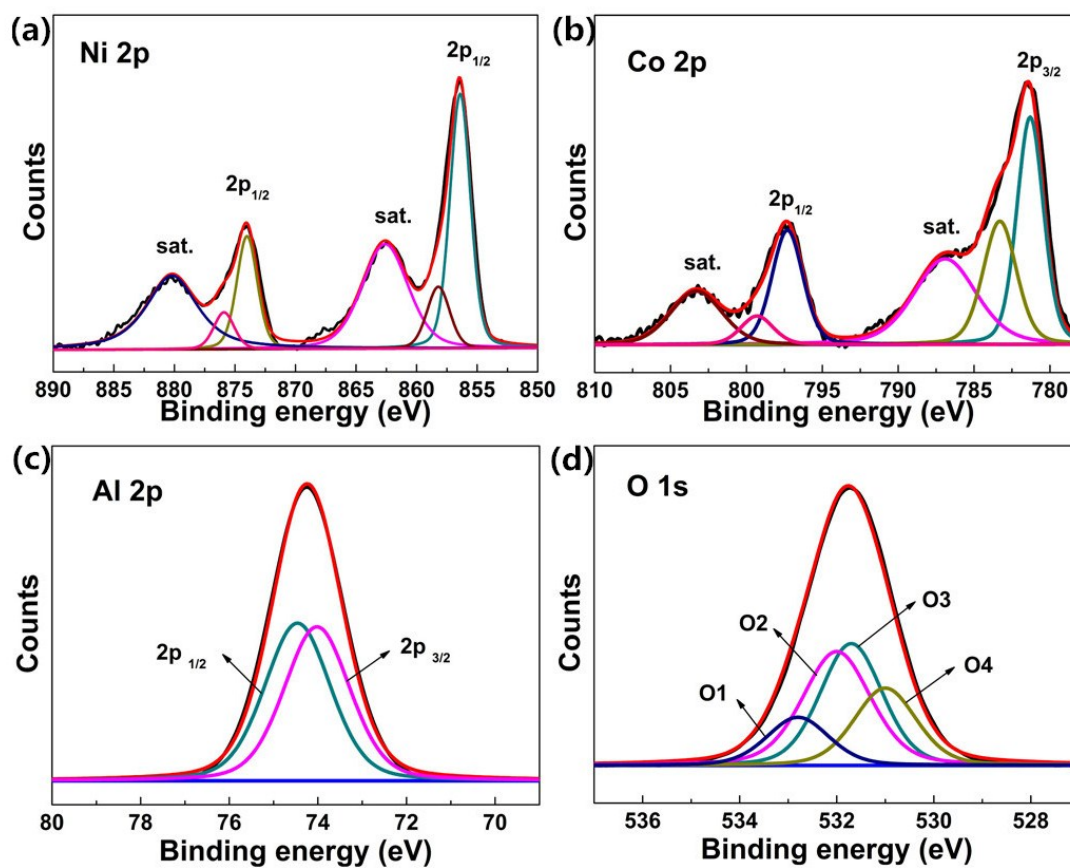


Fig. S8 Fine core-level XPS spectra for Ni 2p (a), Co 2p (b), Al 2p (c) and O 1s(d) peaks of pure m-LDH nanosheets.

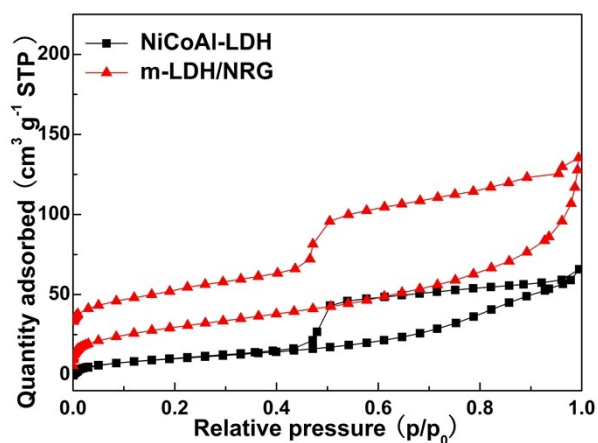


Fig. S9 N_2 adsorption-desorption isothermal plots for m-LDH/NRG NHs and the unmodified NiCoAl-LDH nanosheets.

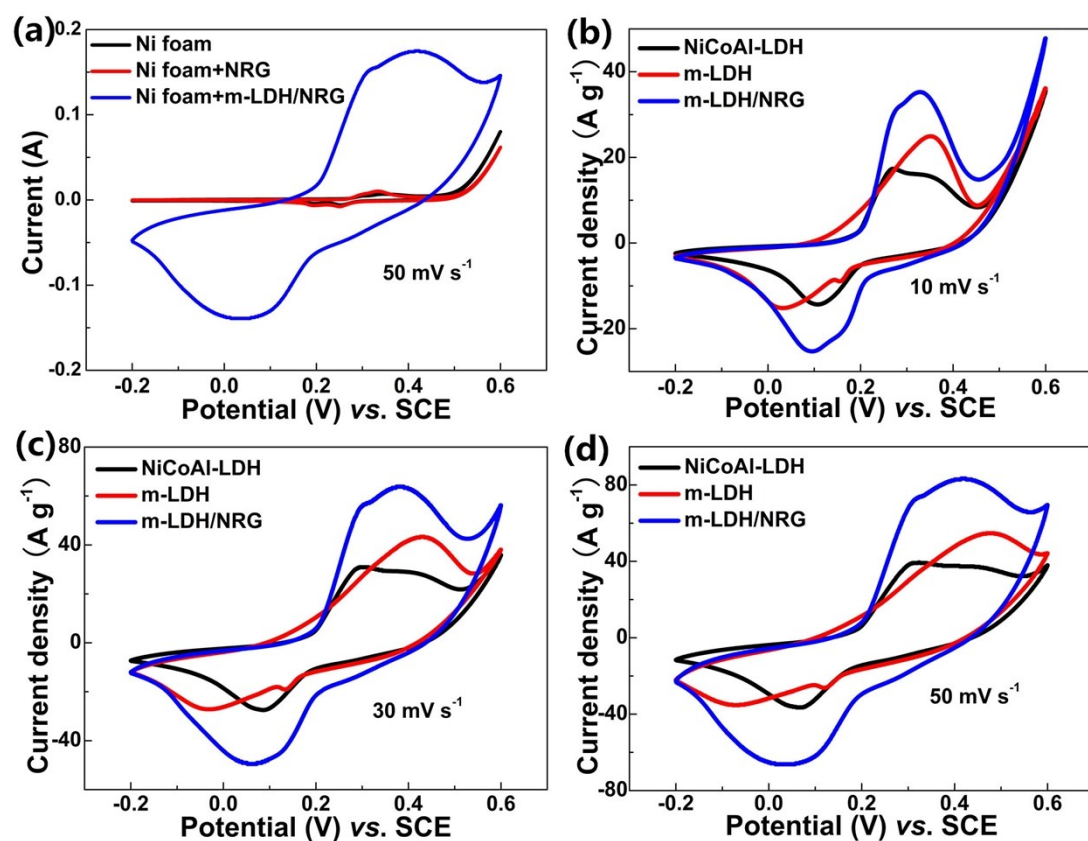


Fig. S10 (a) Comparing the CV curves of m-LDH/NRG NHs with that of pure NRG nanosheets and pure Ni foam at the potential scan rate of 50 mV s⁻¹. (b-d) Comparing the CV curves of m-LDH/NRG NHs with that of NiCoAl-LDH and m-LDH nanosheets at the potential scan rate of 10, 30 and 50 mV s⁻¹, respectively.

Table S1 The detailed data for fitting the Ni 2p, Co2p, Al 2p and O1s fine XPS spectra of m-LDH/NRG NHs, pure m-LDH and unmodified NiCoAl-LDH

| | Spin-orbit | LDH | m-LDH | m-LDH/NRG |
|----|----------------------|---------|---------|-----------|
| Ni | 2p _{1/2} +2 | 856.2eV | 856.5eV | 856.8eV |
| | 2p _{1/2} +3 | 858.1eV | 858.2eV | 858.3eV |
| | 2p _{3/2} +2 | 873.7eV | 874.0eV | 874.4eV |
| | 2p _{3/2} +3 | 875.6eV | 875.9eV | 876.5eV |
| Co | 2p _{1/2} +2 | 783.7eV | 783.3eV | 783.9eV |
| | 2p _{1/2} +3 | 781.2eV | 781.3eV | 781.8eV |
| | 2p _{3/2} +2 | 798.7eV | 799.3eV | 800.1eV |
| | 2p _{3/2} +3 | 796.9eV | 797.3eV | 797.8eV |
| Al | 2p _{1/2} | 73.9eV | 74.0eV | 74.7eV |
| | 2p _{3/2} | 74.3eV | 74.4eV | 75.2eV |
| O | O ₁ | 532.8eV | 532.8eV | 533.6eV |
| | O ₂ | 532.1eV | 532.1eV | 532.6eV |
| | O ₃ | 531.7eV | 531.7eV | 532.2eV |
| | O ₄ | 531.1eV | 531.1eV | 531.6eV |

Table S2 ICP test results for the content of Co, Al and Ni in NiCoAl-LDH and m-LDH nanosheets

| Sample | Element | Ion concentration ($\mu\text{g mL}^{-1}$) | Mass percent |
|------------|---------|---|--------------|
| NiCoAl-LDH | Co | 0.703 | 7.0% |
| | Al | 0.415 | 4.2% |
| | Ni | 2.061 | 20.6% |
| m-LDH | Co | 0.592 | 5.9% |
| | Al | 0.314 | 3.1% |
| | Ni | 1.839 | 18.4% |

[Notes]: For ICP tests, the NiCoAl-LDH and m-LDH nanosheets with the same mass were dissolved in 6 mL concentrated nitric acid, respectively. Then, these solution were added into 100 mL flask and diluted to 100 mL, respectively. The content of various metal elements were examined by ICP.

Table S3. The detailed integral areas of O1s peaks for NiCoAl-LDH and m-LDH nanosheets

| peaks | NiCoAl-LDH (integration area) | m-LDH (integration area) |
|---------------------|----------------------------------|-----------------------------|
| O1 H ₂ O | 26204 | 45757 |
| O2 O-H | 65340 | 121574 |
| O3 oxygen vacancies | 44633 | 114272 |
| O4 M-OH | 107492 | 73501 |

[Notes]: By calculating from their integration areas, the content of O3 peak (O vacancies or defects) in m-LDH nanosheets (about 32.2%) is much higher than that of unmodified NiCoAl-LDH nanosheets (18.3%), implying that etching Al atoms can create more oxygen vacancies in m-LDH in relative to unmodified NiCoAl-LDH. This is consistent with previously reported works (*e.g.*, *Chem. Eur. J.* **2016**, 22, 4000).

Table S4 Comparing the electrochemical performance of m-LDH/NRG NHs with other reported electrode materials

| Electrode materials | Specific capacitance (F g ⁻¹) | Rate performance | Capacitance retention (cycles) | Literatures |
|--|---|-----------------------------|--------------------------------|-------------|
| NiCoAl-LDH/ NRG | 1877 (1 A g ⁻¹) | 72% (10 A g ⁻¹) | 74% (5000) | This work |
| NiAl-LDH/rGO | 1630 (1 A g ⁻¹) | 17% (10 A g ⁻¹) | 95% (1500) | Ref S1 |
| CoMn-LDH/ rGO | 1635 (1 A g ⁻¹) | 71% (10 A g ⁻¹) | 100% (10000) | Ref S2 |
| 3D NiCoMn -LDH/rGO | 912 (1 A g ⁻¹) | 81% (10 A g ⁻¹) | 64% (5000) | Ref S3 |
| CNT@NiCo ₂ O ₄ | 1038 (0.5 A g ⁻¹) | 64% (10 A g ⁻¹) | 100% (1000) | Ref S4 |
| CoAl-LDH/rGO | 825 (1 A g ⁻¹) | 62% (8 A g ⁻¹) | 89% (4000) | Ref S5 |
| Ni _{1-x} Co _x Al- LDH/rGO | 1902 (1 A g ⁻¹) | 75% (10 A g ⁻¹) | 62% (1500) | Ref S6 |
| Ni _x Co _{1-x} S ₈ | 1404 (2 A g ⁻¹) | 38% (9A g ⁻¹) | 75% (2000) | Ref S7 |
| α-(Ni/Co)(OH) ₂ /graphene | 1809 (0.5 A g ⁻¹) | 84% (40 A g ⁻¹) | 83% (1000 0) | Ref S8 |
| NiV-LDH | 1581 (1 A g ⁻¹) | 77% (1 A g ⁻¹) | 40% (10000) | Ref S9 |

| | | | | |
|--|-----------------------------|------------------------------|------------|---------|
| CoAl-LDH@ CoS | 1205 (1 A g ⁻¹) | 941 (10 A g ⁻¹) | 88% (2000) | Ref S10 |
| CoAl-LDH/ graphene | 1296 (1 A g ⁻¹) | 43% ((10 A g ⁻¹) | 90% (1000) | Ref S11 |
| HMCS/Ni(OH) ₂ | 1632 (1 A g ⁻¹) | 61% (10 A g ⁻¹) | 81% (3000) | Ref S12 |
| MoO ₃ /Ni(OH) ₂ | 1622 (1 A g ⁻¹) | 26% (10 A g ⁻¹) | 80% (3000) | Ref S13 |
| Ni(OH) ₂ /3D graphite foam | 1500 (1 A g ⁻¹) | 67% (10 A g ⁻¹) | 65% (1000) | Ref S14 |

[Notes]: The abbreviation of “LDH” stands for the “layered double hydroxides”, and the abbreviation of “NRG” represents “N-doped reduced graphene oxide”. The “rGO” stands for “reduced graphene oxide”.

References

- 1 Y. Wimalasiri, R. Fan. X. S. Zhao, L. Zou, *Electrochim. Acta*, 2014, **134**, 127.
- 2 M. Li, J. P. Chen, J. Wang, F. Liu, X. B. Zhang, *Electrochim. Acta*, 2016, **206**, 108.
- 3 M. Li, J. P. Cheng, F. Liu, X. B. Zhang, *Chem. Phys. Lett.*, 2015, **640**, 5.
- 4 F. Cai, Y. Kang, H. Chen, M. Chen, Q. Li, *J. Mater. Chem. A*, 2014, **2**, 11509.
- 5 Y. Y. Zhong, Y. Q. Liao, A. M. Gao, J. N. Hao, D. Shu, Y. L. Huang, J. Zhong, C. He and R. H. Zeng, *J. Alloys Compd.*, 2016, **669**, 146-155.
- 6 J. Xu, S. L. Gai, F. He, N. Niu, P. Gao, Y. J. Chen, P. P. Yang, *Dalton. Trans.*, 2014, **43**, 11667.
- 7 Y. F. Zhang, C. C. Sun, H. Q. Su, W. Huang and X. C. Dong, *Nanoscale*, 2015, **7**, 3155.

- 8 Y. Z. Chen, W. K. Pang, H. H. Bai, T. F. Zhou, Y. N. Liu, S. Li and Z. P. Guo, *Nano Lett.*, 2017, **17**, 429.
- 9 A. Tyagi, M. C. Joshi, A. Shah, V. K. Thakur and R. K. Gupta, *ACS Omega*, 2019, **4**, 3257.
- 10 Y. B. Dou, J. Zhou, F. Yang, M. J. Zhao, Z. R. Nie and J. R. Li, *J. Mater. Chem. A*, 2016, **4**, 12526.
- 11 Z. C. Huang, S. L. Wang, J. P. Wang, Y. M. Yu, J. J. Wen and R. Li, *Electrochim. Acta*, 2015, **152**, 117.
- 12 Y. S. Fu, Y. Zhou, Q. Peng, C. Y. Yu, Z. Wu, J. W. Sun, J. W. Zhu and X. Wang, *J. Power Sources*, 2018, **402**, 43.
- 13 L. L. Zhu, C. K. N. Peh, T. Zhu, Y. F. Lim and G. W. Ho, *J. Mater. Chem. A*, 2017, **5**, 8343-8351.
- 14 J. Y. Ji, L. L. Zhang, H. X. Ji, Y. Li, X. Zhao, X. Bai, X. B. Fan, F. B. Zhang and R. S. Ruoff, *ACS Nano*, 2013, **7**, 6237-6243.